

Tunable negative coefficient microwave photonic filter based on a polarization modulator and a polarization beam interferometer

Yanbing Jin (金岩冰)¹, Erwin H. W. Chan², Xinhuan Feng (冯新焕)¹,
Xudong Wang (王旭东)^{1,*}, and Bai-ou Guan (关柏鸥)¹

¹Institute of Photonics Technology, Jinan University, Guangzhou 510632, China

²School of Engineering and Information Technology, Charles Darwin University, Darwin, NT 0909, Australia

*Corresponding author: txudong.wang@email.jnu.edu.cn

Received October 20, 2014; accepted February 12, 2015; posted online March 23, 2015

A new tunable microwave photonic notch filter with negative coefficients is presented. It is based on a polarization modulator and a polarization beam interferometer. Experimental results are presented that embody the new concept.

OCIS codes: 060.5625, 070.2615, 230.0250.

doi: 10.3788/COL201513.050601.

Implementation of microwave signal processing in the optical domain has been a topic of interest in the past 2 decades due to the advantageous features provided by photonics such as low loss, light weight, broad bandwidth, large tunability, and insensitivity to electromagnetic interference^[1].

Many photonic signal processor filter structures have been reported^[2-9]. Microwave photonic notch filters with negative coefficients are of interest due to their ability of filtering out the DC component. Several negative-coefficient microwave photonic notch filter structures have been proposed^[6-9]. However, they either suffer from a low signal-to-noise ratio (SNR) caused by the high signal spontaneous beat noise generated by the semiconductor optical amplifier used in the setup^[6], require a complex structure^[7], have the bias drift problem due to the use of an intensity modulator^[8], or have the difficulty to realize the tuning operation^[9]. In this Letter, we propose a new continuously tunable microwave photonic notch filter that has the ability to generate a negative-coefficient frequency response.

The structure of the novel microwave photonic notch filter is shown in Fig. 1. A linearly polarized light from a laser source is launched to a polarization modulator (PolM) with an angle of $\pm 45^\circ$ to one principal axis E_x of the PolM. The PolM is driven by an input RF signal and is operated as an electrically variable wave plate. It can change the polarization state of a linearly polarized laser light to either an orthogonal linear polarization state, an elliptical, or circular polarization state^[9]. The polarization-modulated optical signal at the output of the PolM passes through a polarization beam interferometer (PBI), formed by a polarization beam splitter (PBS) and a polarization beam combiner (PBC) connected in series via polarization maintaining fibers. It should be noted that both the PBS and the PBC are oriented at an angle of 45° to the E_x axis of the PolM. The polarization-modulated

optical signal is split and combined in the PBI orthogonally, and hence there is no coherent interference and no phase-induced intensity noise generation. The output optical signals after the PBI are detected by a photodetector. It should be noted that there is a fiber length difference ΔL between the upper and lower paths of the PBI. This introduces different RF phases to the polarization-modulated optical signals, and since the PolM supports phase modulation on both transverse electric (TE) and transverse magnetic (TM) modes with an opposite modulation index^[10], a negative-coefficient notch filter response can be generated after photodetection.

We assume the continuous-wave light into the PolM is aligned at an angle of 45° to the E_x -axis of the PolM. The electric field at the output of the PolM can be expressed as^[10]

$$E(t) = \begin{bmatrix} E_x(t) \\ E_y(t) \end{bmatrix} \propto \frac{\sqrt{2}}{2} \begin{bmatrix} \exp j(\omega_0 t + \beta \sin \omega_{RF} t) \\ \exp j(\omega_0 t - \beta \sin \omega_{RF} t) \end{bmatrix}, \quad (1)$$

where $E_x(t)$ and $E_y(t)$ are the electric fields of the E_x - and E_y -axis of the PolM, respectively; ω_0 is the angular frequency of the optical carrier; ω_{RF} is the input RF signal angular frequency; $\beta = \pi V_{RF} / V_\pi$ is the phase modulation index of the PolM; V_{RF} is the input RF voltage to the PolM; V_π is the PolM switching voltage. The PBS splits the polarization-modulated optical signal into two paths orthogonally. Since the PBS is oriented at an angle of 45°

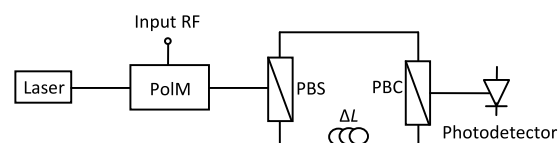


Fig. 1. Topology of the novel microwave photonic notch filter.

to the E_x -axis of the PolM, the electric fields after the PBS can be expressed as

$$\begin{bmatrix} E_{\text{up}}(t) \\ E_{\text{down}}(t) \end{bmatrix} \propto \frac{1}{2} \begin{bmatrix} E_x(t) + E_y(t) \\ -E_x(t) + E_y(t) \end{bmatrix}, \quad (2)$$

where $E_{\text{up}}(t)$ and $E_{\text{down}}(t)$ are the electric fields in the upper and lower arms of the PBS, respectively. A time delay τ is introduced due to the fiber length difference ΔL when the two optical signals with orthogonal polarization state combine at the PBC. Since the two delayed optical signals have an orthogonal polarization state, they combine incoherently at the PBC. Hence the output optical power into the photodetector can be written as

$$P_{\text{out}} \propto |E_{\text{up}}(t)|^2 + |E_{\text{down}}(t - \tau)|^2. \quad (3)$$

Under the condition of small-signal modulation, the transfer function of the notch filter can be obtained from Eq. (3) and is given by

$$H(\omega_{\text{RF}}) \propto 1 - \cos \phi, \quad (4)$$

where $\phi = \omega_{\text{RF}} n \Delta L / c$ is the RF phase difference introduced by the fiber length difference ΔL , n is the fiber refractive index, and c is the speed of light. The free spectral range (FSR) of the notch filter is inversely proportional to the length difference ΔL . Since ΔL can be controlled and can be made very small, the filter has the ability to realize a tuning operation and to achieve a large FSR frequency response. Note that the fiber length difference ΔL between the two paths in the PBI can be tuned while maintaining the light polarization state and without altering the structure. This can be done by inserting a differential group delay module^[1] in the lower path of the PBI. A differential group delay module is commercially available. It does not change the light polarization state, and has over 90 ps tuning range with 1.36 ps resolution. Continuous notch frequency tuning can be realized by inserting a polarization-maintaining optical variable delay line (VDL), which is also commercially available, in the lower path of the PBI. It has 600 ps tuning range and 0.33 ps tuning resolution. Using either a differential group delay module or a polarization maintaining optical VDL to tune the filter notch frequency is flexible and enables a stable performance to be obtained.

The simulated frequency responses of the notch filter are shown in Fig. 2 for $\Delta L = 2.86, 2,$ and 1.54 cm, which correspond to a filter FSR of 7, 10, and 13 GHz, respectively.

It can be seen from Fig. 2 that the frequency response is a two-tap negative tap notch filter response. The PolM- and PBI-based microwave photonic notch filter has the advantage of no bias voltage required for the PolM. The orthogonal polarization delayed optical signals arriving at the photodetector do not interfere with each other so there is no phase noise problem^[2]. Hence, the system has a high SNR performance. A narrow linewidth laser

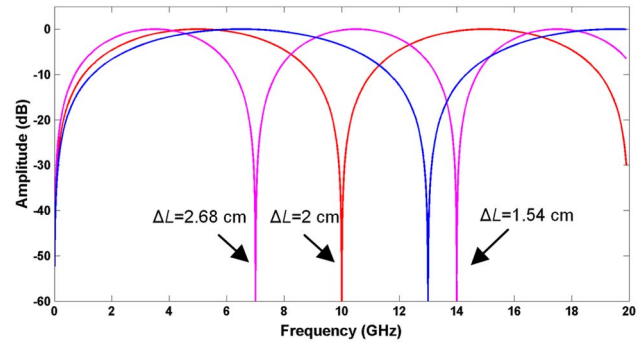


Fig. 2. Normalized frequency response of the PolM- and PBI-based microwave photonic notch filter for different values of ΔL .

can be used as the optical source to generate a stable response insensitive to changes in environmental condition. In other words, the filter has no coherent interference problem. The PolM is operated based on the electro-optic effect and electro-optic modulators with a very wide bandwidth up to 100 GHz have been demonstrated^[3]. Hence the notch filter can be operated at very high frequencies well into the millimeter wave frequency range.

An experiment was set up based on Fig. 1 to verify the principle of the PolM- and PBI-based microwave photonic notch filter. A DFB laser, which had a linewidth of less than 1 MHz, was used as the optical source. A polarization controller (PC) was used after the DFB laser to adjust the polarization state of the continuous-wave light to have an angle of $\pm 45^\circ$ to one principal axis E_x of the PolM. A PBS and a PBC, which were oriented at an angle of 45° to the E_x -axis of the PolM, were used to form the PBI. A VDL with single-mode fiber pigtailed was inserted in the lower path of the PBI. This altered the polarization state of the optical signal and introduced an extra insertion loss in the lower path of the PBI. Therefore, a PC was used in the lower path to align the light polarization state to maximize the efficiency of the PBC. Another PC was placed in the upper path, which was used to control the efficiency of the PBC in the upper path and was functioned as a variable attenuator to match the amplitudes of the two delayed optical signals traveled in the upper and lower path of the PBI. It should be noted that the PCs inside the PBI can be avoided by using a polarization-maintaining VDL and a polarization-maintaining attenuator. After the PBI, the two delayed optical signals were detected by a 50 GHz bandwidth photodetector, connected to a 26.5 GHz bandwidth network analyzer to display the frequency response.

The VDL was set to have a fiber length difference ΔL of 2.63 cm, corresponding to a filter FSR of 7.6 GHz. To demonstrate the continuously tunable notch filtering operation, the VDL was adjusted so that ΔL was 3.52, 4.41, and 8.57 cm, which changed the notch frequency to 5.69, 4.54, and 2.33 GHz, respectively, as shown in Fig. 3. The simulated notch filter responses obtained using Eq. (4) together with the ΔL used in the work are also shown in Fig. 3 for comparison. Excellent agreement

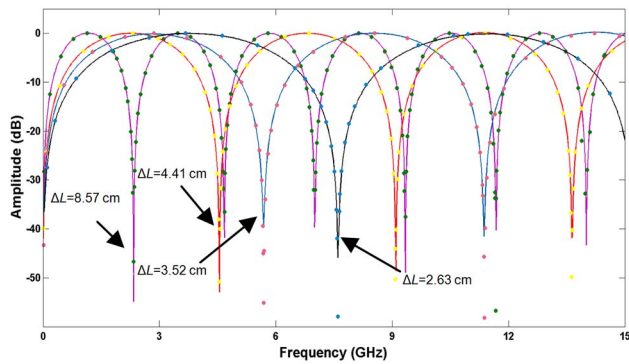


Fig. 3. Simulated (dots) and measured (solid) PolM- and PBI-based microwave photonic notch filter responses for different ΔL values.

between the measured and simulated notch filter responses can be seen. Figure 3 shows the notches have ≥ 40 dB depth while tuning the notch frequency. The filter response was stable, even though the laser linewidth was significantly smaller than the filter FSR, which demonstrated that the filter is free of coherent interference limitations.

The SNR of the notch filter was measured by applying an RF signal at the notch filter passband frequency with an input RF power of 5 dBm to the PolM and an optical power into the photodetector of 0 dBm. An SNR of 118.6 dB/Hz was measured on a spectrum analyzer at the photodetector output. For comparison, a fiber-optic link comprising a laser, an intensity modulator, and a photodetector was set up. The link operating condition, including the RF signal power applied to the modulator and the optical power into the photodetector, was the same as that of the notch filter. An SNR of 119.8 dB/Hz was obtained, which was close to the PolM- and PBI-based notch filter SNR. The high SNR demonstrated that there was no phase-induced intensity noise presented in the filter.

The stability of the PolM- and PBI-based notch filter was investigated experimentally. This was done by measuring the filter frequency response every 15 min for 5 h. The experimental results are shown in Fig. 4. It can be seen from Fig. 4 that the notch filter frequency response is stable for a long period of time. The notch depth was more than 35 dB throughout the measurement period. The notch filter passband amplitude had less than 1 dB variation.

In conclusion, a new single-wavelength, coherence-free microwave photonic notch filter with negative coefficients is presented. It has the ability to generate a large FSR

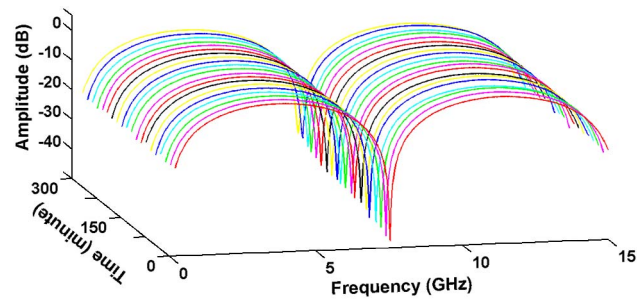


Fig. 4. Frequency responses of the PolM- and PBI-based microwave photonic notch filter measured every 15 min for 5 h.

frequency response, and to operate at high frequencies with wide tunability. The concept is based on a PolM and a PBI with a fiber length difference between the two arms of the PBI. Experimental results demonstrate a negative-coefficient notch filter with a robust frequency response, a large and continuous notch frequency tuning range, and deep notches of ≥ 40 dB.

This work was supported in part by the National Natural Science Foundation of China (No. 61475065), the Natural Science Foundation of Guangdong Province of China (No. S2012010008850), and the Fundamental Research Funds for the Central Universities (No. 21612201) in China.

References

1. R. A. Minasian, E. H. W. Chan, and X. Yi, *Opt. Express* **21**, 22918 (2013).
2. Y. Yu, X. Zheng, H. Zhang, and B. Zhou, *Chin. Opt. Lett.* **11**, 120601 (2013).
3. D. Zou, X. Zheng, S. Li, H. Zhang, and B. Zhou, *Chin. Opt. Lett.* **12**, 080601 (2014).
4. Y. Stern, K. Zhong, T. Schneider, R. Zhang, Y. Ben-Ezra, M. Tur, and A. Zadok, *Photon. Res.* **2**, B18 (2014).
5. E. H. W. Chan and R. A. Minasian, *IEEE Photon. Technol. Lett.* **18**, 1252 (2006).
6. X. Li, E. Xu, L. Zhou, Y. Yu, J. Dong, and X. Zhang, *Opt. Commun.* **283**, 3026 (2010).
7. Y. M. Chang, J. Lee, and J. H. Lee, *Appl. Opt.* **50**, 329 (2011).
8. J. Capmany, D. Pastor, A. Martinez, B. Ortega, and S. Sales, *Opt. Lett.* **28**, 1415 (2003).
9. J. P. Yao and Q. Wang, *IEEE Photon. Technol. Lett.* **19**, 644 (2007).
10. A. L. Campillo, *Opt. Lett.* **32**, 3152 (2007).
11. J. X. Chen, Y. Wu, J. Hodiak, and P. K. L. Yu, *IEEE Photon. Technol. Lett.* **15**, 284 (2003).
12. M. Tur and E. L. Goldstein, *Opt. Lett.* **15**, 1 (1990).
13. H. Huang, S. R. Nuccio, Y. Yue, J. Y. Yang, Y. Ren, C. Wei, G. Yu, R. Dinu, D. Parekh, C. J. Chang-Hasnain, and A. E. Willner, *IEEE Photon. Technol. Lett.* **30**, 3647 (2012).